

A UNIFIED PICTURE FOR LOW-LUMINOSITY AND LONG GAMMA-RAY BURSTS BASED ON THE EXTENDED PROGENITOR OF *l*GRB 060218/SN 2006AJ

EHUD NAKAR¹

Draft version September 8, 2021

ABSTRACT

The relation between long gamma-ray bursts (LGRBs) and low-luminosity GRBs (*l*GRBs) is a long standing puzzle – on the one hand their high energy emission properties are fundamentally different, implying a different gamma-ray source, yet both are associated with similar supernovae of the same peculiar type (broad-line Ic), pointing at a similar progenitor and a similar explosion mechanism. Here we analyze the multi-wavelength data of the particularly well-observed SN 2006aj, associated with *l*GRB 060218, finding that its progenitor star is sheathed in an extended ($> 100R_{\odot}$), low-mass ($\sim 0.01M_{\odot}$) envelope. This progenitor structure implies that the gamma-ray emission in this *l*GRB is generated by a mildly relativistic shock breakout. It also suggest a unified picture for *l*GRBs and LGRBs, where the key difference is the existence of an extended low-mass envelope in *l*GRBs and its absence in LGRBs. The same engine, which launches a relativistic jet, can drive the two explosions, but, while in LGRBs the ultra-relativistic jet emerges from the bare progenitor star and produces the observed gamma-rays, in *l*GRBs the extended envelope smothers the jet and prevents the generation of a large gamma-ray luminosity. Instead, the jet deposits all its energy in the envelope, driving a mildly relativistic shock that upon breakout produces a *l*GRB. In addition for giving a unified view of the two phenomena, this model provides a natural explanation to many observed properties of *l*GRBs. It also implies that *l*GRBs are a viable source of the observed extra-galactic diffuse neutrino flux and that they are promising sources for future gravitational wave detectors.

Subject headings: gamma-ray burst: general — gamma-ray burst: individual (GRB060218, GRB980425, GRB031203, GRB100316D) — supernovae: general — supernovae: individual (SN2006aj, SN1998bw, SN2003lw, SN2010bh) — neutrinos — gravitational waves

1. INTRODUCTION

The gamma-ray emission of LGRBs and *l*GRBs show almost no similarities apart from being detected by the same instruments. LGRBs are luminous ($10^{50} - 10^{52}$ erg/s), hard ($\gtrsim 100$ keV), highly variable and narrowly collimated with a typical duration of 10-100 s (Piran 2004, and references therein). *l*GRBs are fainter by about four orders of magnitude ($10^{46} - 10^{48}$ erg/s), relatively soft ($\lesssim 100$ keV), not highly beamed and show no significant temporal variability over their entire duration, which is often longer than 1000 s (Kulkarni *et al.* 1998; Campana *et al.* 2006; Soderberg *et al.* 2006; Kaneko *et al.* 2007).

To date there are only four well observed *l*GRBs², compared to hundreds of LGRBs. However, this is a result of their low luminosity, which limits the detection to a distance of ~ 100 Mpc, compared to LGRBs which are seen through the entire Universe. In fact, *l*GRBs are much more common than LGRBs, and are the most abundant known relativistic explosions in the nearby Universe (Soderberg *et al.* 2006; Pian *et al.* 2006). Thus, *l*GRBs are of special interest, both for the understanding of GRBs and their connection to SNe, and as sources

of high energy non-electromagnetic signals, such as gravitational-waves (e.g., Kotake, Takiwaki & Harikae 2012; Birnholtz & Piran 2013; Ando *et al.* 2013), neutrinos (e.g., Murase *et al.* 2006; Murase & Ioka 2013) and cosmic-rays (e.g., Budnik *et al.* 2008; Liu, Wang & Dai 2011).

Based on high energy emission alone there is no reason to assume that LGRBs and *l*GRBs are related. Moreover, theoretical considerations show that the gamma-rays seen in *l*GRBs cannot be produced in the same environment where the gamma-rays in LGRBs are generated (Bromberg, Nakar & Piran 2011). It is therefore puzzling that these two apparently different GRB types are both associated with very similar peculiar SNe of the rare broad-line Ic type (e.g., Melandri *et al.* 2014). These SNe show no signs of H or He in their spectra, an indication of highly stripped progenitors. Their ejecta have unusually high velocities for SNe (10,000–30,000 km/s), their peak luminosities indicate a relatively large amount of synthesized ⁵⁶Ni, and the total kinetic energy carried by some of these SNe is unusually high (Woosley & Bloom 2006, and references therein). The similarity of the associated SNe suggests that *l*GRBs and LGRBs have similar progenitors and similar inner explosion mechanism. The natural question that arises is how similar explosions produce such different gamma-ray signals.

Here we approach this puzzle by analyzing the early (first day) optical/UV light curve of SN 2006aj, which is associated with *l*GRB 060218, in order to study

¹ Raymond and Beverly Sackler School of Physics and Astronomy, Tel Aviv University, Tel Aviv 69978, Israel

² These are GRBs with luminosity $\lesssim 10^{48}$ erg/s for which an associated SNe was observed - *l*GRB/SN: 980425/1998bw, 031203/2003lw, 060218/2006aj and 100316D/2010bh.

its progenitor structure. *l*GRB 060218/SN 2006aj has the best early observational coverage out of the four well observed *l*GRBs and their associated SNe. It includes Swift continuous gamma-ray, X-ray, UV and optical observations ranging from $10^2 - 10^6$ s after the explosion (Campana *et al.* 2006), many optical spectra starting less than two days after the explosion (Mirabal *et al.* 2006; Modjaz *et al.* 2006; Mazzali *et al.* 2006; Pian *et al.* 2006; Sollerman *et al.* 2006) and radio observations starting a day after the explosion (Soderberg *et al.* 2006). In fact SN 2006aj has probably the most detailed early optical/UV photometric coverage out of the thousands SNe observed to date.

The unique feature of the optical/UV light curve of SN 2006aj is that it shows two peaks. Using a recently developed method for the analysis of double-peaked SNe (Nakar & Piro 2014) we constrain the progenitor properties. These properties are then used to learn about the physics of *l*GRBs and on their relation to LGRBs.

The paper structure is as follows. Section §2 presents the analysis of the optical/UV light curve and the resulting constraints on the progenitor structure of *l*GRB 060218/SN 2006aj. These constraints strongly support the suggestion that *l*GRBs are generated by shock break-outs (§3). A unified picture for *l*GRBs and LGRBs that naturally explain the similarities and differences between them is presented in §4. This picture provides a simple explanation to the unique velocity profile of SNe associated with *l*GRB (§5). The implication of this picture for *l*GRBs’ neutrino and gravitational wave emission is discussed in §6.

2. THE PROGENITOR OF *l*GRB 060218/SN 2006AJ

Figure 1 depicts the optical/UV light curve of SN 2006aj as taken from Campana *et al.* (2006). It shows two peaks in the optical bands, at $t \approx 10$ hr and $t \approx 10$ days, where t is time since first detection of the gamma-rays, estimated here as the explosion time. Such double-peaked light curves are very rare among SNe. In typical SNe the light curve is dominated by one of two power sources: (i) the internal energy deposited by the SN shock, known as “cooling envelope emission”, or (ii) the radioactive decay of ^{56}Ni . Each one of these power sources produces only a single peak in the optical and, in typical SNe, the time scales of the maximal contribution to the optical light from each of the two sources are comparable. Therefore, observed SN light curves usually contain only a single optical peak which is powered by the stronger power source at any given SNe. This is cooling envelope in explosions of red supergiants, such as type II-P SNe, and ^{56}Ni in explosions of more compact progenitors, such as type I and 1987-like SNe.

Two peaks are observed in rare cases where at early time the emission is powered by the cooling envelope, which then decays sharply on a time scale comparable to that of the rising ^{56}Ni contribution. This behavior requires an atypical progenitor structure of a compact massive core that is engulfed by extended low-mass material (Hoflich, Langer & Duschinger 1993; Bersten *et al.* 2012; Nakar & Piro 2014). The second peak in these cases is similar to the main peak of a typical ^{56}Ni powered SNe, and thus its properties provide an estimate of the total ejecta mass and of the ^{56}Ni mass. In the case

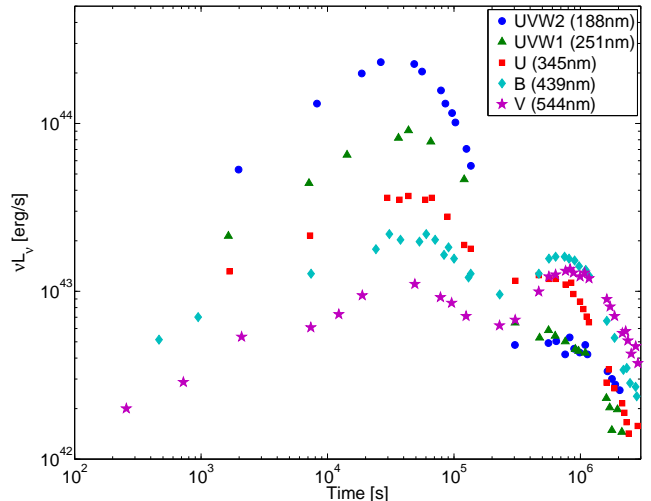


FIG. 1.— Swift UVOT light curve of SN 2006aj in five filters (central wavelength given in the legend) from Campana *et al.* (2006). Following Campana *et al.* (2006) the light curve is corrected for Galactic reddening, $E(B-V) = 0.14$ (assuming a Galactic reddening curve with $R_V = 3.1$), and a host galaxy reddening $E(B-V) = 0.20$ (assuming a Small Magellanic Cloud reddening curve).

of SN 2006aj the second peak is clearly powered by ^{56}Ni and it shows a total ejecta mass of $\sim 2 M_\odot$, out of which $\sim 0.2 M_\odot$ are ^{56}Ni (Mazzali *et al.* 2006). The only natural source of the first peak in SN 2006aj is the cooling envelope phase of an extended mass (see appendix A) and thus its properties can provide a robust estimate of the radius and the mass of the extended material. Here the results of Nakar & Piro (2014) are used to derive these constraints.

The mass of the extended material can be estimated from the time of the first peak, t_p (Nakar & Piro 2014):

$$M_{ext} \approx 0.01 \frac{v_{ext}}{0.2c} \left(\frac{t_p}{10 \text{ hr}} \right)^2 M_\odot \quad (1)$$

where c is the light speed and v_{ext} is the velocity to which the extended material is accelerated by the explosion. Spectroscopic observations limit $v_{ext} > 0.1c$, the measured photospheric velocity at $t = 2.89$ day (Pian *et al.* 2006). On the high end it is most likely that $v_{ext} < 0.3c$, since at higher velocity the kinetic energy carried by M_{ext} would be larger than the kinetic energy deposited by the explosion in the massive core ($\sim 10^{51}$ erg; Mazzali *et al.* 2006).

The pre-explosion radius of the extended material, R_{ext} , can be estimated by the bolometric luminosity at the first peak. The colors before and during the first peak are very blue and they are constant in time (Simon, Pizzichini & Hudec 2010), as expected if the observed bands are on the Rayleigh-Jeans part of a black-body spectrum during that time (i.e., with temperature $T(t \leq t_p) \gtrsim 50,000$ K; see consistency check below). This implies that the total luminosity seen in UV during the peak, $\sim 3 \cdot 10^{44}$ erg, is only a lower limit on the true bolometric luminosity, which may be significantly higher. Since R_{ext} is linear in the bolometric luminosity (Nakar & Piro 2014), the available observations set a

lower limit:

$$R_{ext} \gtrsim 10^{13} \left(\frac{v_{ext}}{0.2 c} \right)^{-2} \text{ cm} \quad (2)$$

This is consistent with the lack of color evolution at $t < t_p$ and the model prediction that temperature is dropping with time, reaching at the peak $T(t_p) \approx 50,000(R_{ext}/10^{13} \text{ cm})^{1/4} \text{ K}$ (Nakar & Piro 2014). Thus, the optical/UV light curve of SN 2006aj indicates that its progenitor had a relatively compact core of several solar masses, surrounded by $\sim 0.01 M_\odot$ which is extended to a radius of a supergiant. This structure is very different than the typically expected structure of a fully H stripped progenitor, based on stellar evolution models, yet it must be very common in GRB progenitors given that ll GRBs are more common than LGRBs. This progenitor structure has several far reaching implications for the physics of ll GRBs and their associated SNe, which are discussed in the following sections.

3. SHOCK BREAKOUT ORIGIN FOR ll GRBs

The Thomson optical depth of the extended material is high, $\sim 3,000(R_{ext}/10^{13} \text{ cm})^{-2}$. As a result, the breakout of the shock driven by the explosion takes place at R_{ext} . Radio observations show that the leading edge of the outflow is mildly relativistic (Soderberg *et al.* 2006), implying that the breakout must be at least at a mildly relativistic velocity, i.e., $v_{bo} \gtrsim 0.5 c$. Since rate considerations indicate that the gamma-rays in ll GRBs are not strongly beamed (Soderberg *et al.* 2006) and late SN spectroscopy and polarimetry show no signs of ejecta a-sphericity (Mazzali *et al.* 2007), the breakout is not expect to strongly deviate from a spherical symmetry. In that case the main characteristics of a mildly relativistic shock breakout signal, its luminosity, duration and typical photon energy, depend only on the breakout radius (Nakar & Sari 2012):

$$\begin{aligned} L_{bo} &\sim 2 \cdot 10^{46} \frac{R_{ext}}{3 \cdot 10^{13} \text{ cm}} \text{ erg s}^{-1} \\ t_{bo} &\sim 1000 \frac{R_{ext}}{3 \cdot 10^{13} \text{ cm}} \text{ s} \\ T_{bo} &\sim 50 \text{ keV} \end{aligned} \quad (3)$$

This is similar to the actual gamma-ray signal of ll GRB 060218 where $L_{bo,obs} \approx 3 \cdot 10^{46} \text{ erg s}^{-1}$, $t_{bo,obs} \approx 1,000 \text{ s}$ and $T_{bo,obs} \approx 40 \text{ keV}$ (Kaneko *et al.* 2007) and it fits very well to a breakout radius $R_{ext} \sim 3 \cdot 10^{13} \text{ cm}$. Thus, the combination of optical/UV and radio observations imply that a shock breakout signal is inevitable and that its properties are similar to the observed ll GRB. As shock breakout also explains a large range of properties of the high energy emission from ll GRBs (e.g., smooth profile, spectral evolution, low beaming; Nakar & Sari 2012), this result practically implies that the entire gamma-ray signal in ll GRB 060218 is generated by a mildly relativistic shock breakout, without any significant contribution from a relativistic jet. It also lends a very strong support for the suggestion that all ll GRBs are shock breakouts (Kulkarni *et al.* 1998; Tan, Matzner & McKee 2001; Campana *et al.* 2006; Waxman, Mészáros & Campana 2007; Li 2007; Katz, Budnik & Waxman 2010; Nakar & Sari 2012).

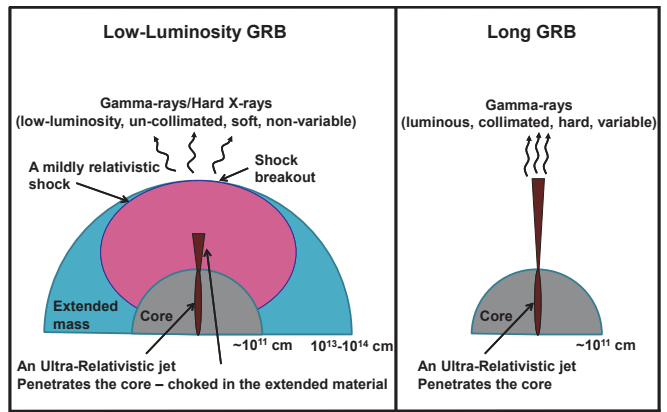


FIG. 2.— A schematic sketch illustrating the similarity and differences between ll GRBs and LGRBs. Both explosions go through a collapse of a similar core which leads to the formation of a similar GRB engine and to a similar SN explosion. In both types the GRB engine launches ultra-relativistic narrowly collimated jet, which penetrates through the core. In LGRBs the jet is free to expand as soon as it is out of the core where it produces a luminous, hard, narrowly collimated beam of gamma-rays which can vary in time on short time scales. In ll GRB the jet emerges from the core into the low-mass extended material where it is choked and any radiation that it produces is absorbed and cannot reach to the observer. The jet energy is deposited in the extended material driving a strong shock into it. The shock is much less relativistic than the jet (most likely Newtonian) and it accelerates before breakout (often to a mildly relativistic velocity). Upon breakout it produces low-luminosity soft gamma-rays which show no significant variability with time and are not narrowly beamed.

4. A UNIFIED PICTURE FOR LGRBS AND ll GRBs

If all ll GRB progenitors have a similar structure to that of ll GRB 060218 then it provides a natural solution to the puzzle why two explosions with similar inner workings produce such different gamma-ray signals. According to the standard model for LGRBs the burst is powered by a central engine that launches a highly collimated ultra-relativistic bipolar jet. In order to produce a LGRB the jet must first punch its way through the star and then expand freely at ultra-relativistic velocities to radii where generated gamma-rays can be seen by the observer. While the jet drills through the dense stellar matter its energy is dissipated and the engine must continue to supply power into the jet if it is to succeed punching through the star and produce the observed LGRB (Zhang, Woosley & MacFadyen 2003; Morsony, Lazzati & Begelman 2007; Mizuta & Aloy 2009; Bromberg *et al.* 2011). Thus, a necessary condition for the production of a LGRB is that the engine working time is long enough to allow the jet to drill through the star. Observations indicate that a typical LGRB engine launches a jet at a typical isotropic equivalent luminosity of $L_{iso} \sim 10^{51} \text{ erg/s}$ and a typical opening angle $\theta_j \sim 10^\circ$ over a typical duration of $\sim 20 \text{ s}$ (Piran 2004). The total energy carried by the jet, after correction for beaming, is $\sim 10^{51} \text{ erg}$. If the progenitor is a bare H stripped star of several solar masses and several solar radii it takes $\sim 10 \text{ s}$ for the jet to penetrate through the star (see appendix B; Bromberg *et al.* 2011), implying that the jet can successfully emerge from the star and that the collapse of such a progenitor can lead to a LGRB.

The picture, however, is very different if there is an additional extended envelope surrounding the massive

core, similar to the one found here for \llcorner GRB 060218. Although the extended material mass is low its large radius makes it very hard for a jet to penetrate. In fact the time that the engine must work in order for the jet to drill through the entire extended mass is (appendix B):

$$t_{eng} \gtrsim 150 \left(\frac{L_{iso}}{10^{51} \text{erg/s}} \right)^{-\frac{1}{2}} \left(\frac{R_{ext}}{3 \times 10^{13} \text{cm}} \right)^{\frac{1}{2}} \left(\frac{M_{ext}}{10^{-2} M_{\odot}} \right)^{\frac{1}{2}} \text{ s.} \quad (4)$$

This time is considerably longer than the typical working time of a LGRB engine. Thus, a collapse of the progenitor of \llcorner GRB 060218 and the formation of a LGRB engine at its center will not lead to an observed LGRB. Instead, the launched jet, which penetrates the stellar core, is choked while still propagating in the extended material. The energy carried by the jet ($E_{jet} \sim 10^{51}$ erg) is then deposited in the extended mass accelerating

it to high velocity ($v_{ext} \approx 0.3c \left[\frac{E_{jet}}{10^{51} \text{erg}} \right]^{\frac{1}{2}} \left[\frac{M_{ext}}{10^{-2} M_{\odot}} \right]^{-\frac{1}{2}}$) and driving into it a strong shock. The shock accelerates further at the dropping density gradient near R_{ext} and upon breakout produces a \llcorner GRB.

Note that while the energy deposition is done by a narrow jet and is therefore highly aspherical, the shock upon breakout can be quasi-spherical. The reason is that the jet is choked long before it approaches R_{ext} and the resulting blast wave becomes much more spherical during its propagation before it breaks out at R_{ext} . A schematic sketch of the similarities and differences between \llcorner GRBs and LGRBs according to this picture is illustrated in figure 2.

5. THE UNCOMMON VELOCITY PROFILE OF SNE ASSOCIATED WITH \llcorner GRBs

This scenario resolves yet another puzzle related to SNe associated with \llcorner GRBs – why is the kinetic energy in their fast moving ejecta is so high compared to other SNe (Soderberg *et al.* 2006). In typical SNe the explosion energy is all deposited at the center of the progenitor. This drives a shock that crosses first the bulk of the mass and then accelerates at the sharp density drop near the stellar edge. This acceleration dictates a certain relation between the kinetic energy carried by slow and by fast moving material, where $E_k(v) \propto v^{-5}$ (Sakurai 1960; Matzner & McKee 1999). This relation is seen in regular SNe, but not in \llcorner GRBs where the fast moving ejecta carries much more energy than it predicts (Soderberg *et al.* 2006). For example, in SN 2006aj about 2×10^{51} erg are carried by the bulk of the mass at $\sim 10,000$ km/s (Mazzali *et al.* 2006). In a regular SNe if a mildly relativistic ($> 150,000$ km/s) ejecta exist, the relation $E_k(v) \propto v^{-5}$ dictates that it should carry $\sim 2 \times 10^{45}$ erg. Instead, in SN 2006aj radio observations indicate that the mildly relativistic material carries $\gtrsim 10^{48}$ erg (Soderberg *et al.* 2006; Barniol Duran *et al.* 2014). This observed property of SN 2006aj is naturally explained by the picture of \llcorner GRBs presented here. In this picture the energy in the slow moving material is deposited by the SN explosion mechanism at the center, while the observed $> 10^{48}$ erg in the fast moving material is deposited directly by a GRB jet, thereby decoupling the amount of energy carried by each of the components.

6. NEUTRINOS AND GRAVITATIONAL WAVES FROM \llcorner GRBs

An intriguing implication of the arising picture is the prospects for future detection of non-electromagnetic signal from \llcorner GRBs. The extreme energies and velocities involved in LGRB engines and jets make them a potential source of gravitational waves (GW), neutrinos and high-energy cosmic rays. However LGRBs are very rare in the local Universe and are typically seen at a distance $> \text{Gpc}$. Here we suggest that \llcorner GRBs harbor the same engine as LGRBs, which produces similar ultra-relativistic jets. The propagation of an \llcorner GRB jet is similar to that of a LGRB jet within the massive core. After the jet breaks out of the core and into the \llcorner GRB extended envelope the envelope density is low, so the pressure in the cocoon does not affect the jet (see appendix B). Thus, at any location that is far from the jet head the jet is unaware of the extended envelope. Therefore, all the physical processes that take place during the formation of the engine, the launching of the jet and the jet propagation in LGRB also take place in \llcorner GRBs up to the radius where \llcorner GRB jets are choked in their progenitors' extended envelopes, namely $\sim 10^{12} - 10^{13}$ cm. Thus, the same emission generated by a LGRB engine and by its jet while it propagates up to a radius of $\sim 10^{12} - 10^{13}$ cm are expected to be generated also by a \llcorner GRB. This includes photons, high energy particles (cosmic-rays), neutrinos and GWs. The extended envelope has a Thompson optical depth $\gg 100$ and therefore photons and cosmic-rays cannot escape through the extended envelope (the cross-section for pp inelastic collision at $\sim \text{TeV}$ energies is ~ 0.1 Thomson). However, the envelope is transparent to neutrinos and GWs. It is therefore worth considering the implications of the model presented here for neutrino and GW emission from \llcorner GRBs, especially given that \llcorner GRBs are more common than LGRBs.

LGRBs are expected to be bright sources of high energy neutrinos ($\sim 10^{14} - 10^{16}$ eV). The most promising production site of neutrinos is internal shocks within the relativistic jet (Waxman & Bahcall 1997). At radii that are large enough $> 10^{11} - 10^{12}$ cm these shocks are collisionless and are therefore expected to efficiently accelerate protons (at smaller radii the shocks are radiation mediated and no efficient particle acceleration is expected; Levinson & Bromberg 2008). At radii that are small enough, $\lesssim 10^{14}$, the photon density is high enough to allow an efficient photo-pion production and thus a generation of high energy neutrinos. Current measurements limit the neutrino flux from LGRBs to $E_0^2 \phi_0 \lesssim 2 \times 10^{10} \text{ GeV cm}^{-2} \text{ s}^{-1} \text{ sr}^{-1}$ per flavor, where $E_0 = 100 \text{ TeV}$ (Aartsen *et al.* 2014). This upper limit is comparable to recent estimates of the flux expected from LGRBs if particles are accelerated efficiently in internal shocks at radii of $\sim 10^{12} - 10^{14}$ cm (Hümmer, Baerwald & Winter 2012) and it is about two order of magnitude lower than the measured diffuse neutrino flux (Aartsen *et al.* 2014).

In the picture presented here \llcorner GRBs are expected to be a much stronger source of diffuse neutrino flux than LGRBs³. First \llcorner GRBs are more numerous. The lo-

³ Note that in the model discussed here the neutrinos are generated in a different environment than in the model discussed by Murase & Ioka (2013), where they assume that \llcorner GRBs are generated by internal shocks in a wide mildly-relativistic low-luminosity

cal rate of \mathcal{L} GRBs, without correction for beaming, is $\sim 3 \times 10^{-7} \text{ Mpc}^{-3} \text{ yr}^{-1}$, where beaming correction is expected to be relatively small, < 10 (Soderberg *et al.* 2006; Pian *et al.* 2006). This is compared to a LGRB local rate, uncorrected for beaming, of $\sim 10^{-9} \text{ Mpc}^{-3} \text{ yr}^{-1}$ (Wanderman & Piran 2010). Beaming correction increases the true rate of LGRBs by about two orders of magnitude. Thus, \mathcal{L} GRBs are more frequent than LGRBs by about an order of magnitude. Second, The neutrino production of LGRBs depends on the fraction of high-energy protons that produce pions via interaction with the observed gamma-rays. This fraction, denoted as f_π , depends strongly on the burst parameters and it vary between bursts. Under optimal conditions the estimates are $f_\pi \lesssim 0.1$ (Waxman & Bahcall 1997; Hümmer, Baerwald & Winter 2012). In \mathcal{L} GRBs however, the jet is buried in an envelope that is optically thick to high-energy protons. Thus, energy of protons that in LGRBs would have been released to the host galaxy as cosmic-rays is converted in large part to neutrinos via pp interactions. Thus, assuming that a large fraction of the LGRBs' neutrinos are generated at radii smaller than $\sim 10^{13} \text{ cm}$, \mathcal{L} GRBs are more efficient in producing $\sim 100 \text{ TeV}$ neutrinos by about two orders of magnitude, and possibly more (this is the product of the \mathcal{L} GRB to LGRB rate ratio and $1/f_\pi$).

As high-energy protons are accelerate within the ultra-relativistic narrowly collimated jets, the neutrino signal is narrowly beamed as well. Since the gamma-ray emission from \mathcal{L} GRBs is not highly beamed, most of observed bursts are not expected to be accompanied by a neutrino signal. Thus, \mathcal{L} GRBs will contribute to the diffuse flux but they are not suitable for a targeted point-sources search, similar to the search conducted for LGRBs (Aartsen *et al.* 2014). Can \mathcal{L} GRBs be then the main source of the observed diffuse flux? Ahlers & Halzen (2014) find that the sources of the diffuse neutrino flux produce a total energy output of $\sim 10^{43} \text{ erg Mpc}^{-3} \text{ yr}^{-1}$ in $\sim 100 \text{ TeV}$ neutrinos and their volumetric rate, assuming transient sources, must be $\gtrsim 10^{-8} \text{ Mpc}^{-3} \text{ yr}^{-1}$ (as inferred from the lack of neutrino clustering). Assuming that each \mathcal{L} GRB harbor a relativistic jet with a typical energy of $\sim 10^{51} \text{ erg}$ the total energy output in such jets is $\sim 3 \times 10^{44} \text{ erg Mpc}^{-3} \text{ yr}^{-1}$. Thus, if $\sim 10\%$ of this energy is converted to high-energy protons before the jet is choked (i.e., at radii $\lesssim 10^{13} \text{ cm}$) then \mathcal{L} GRBs are producing the observed diffuse flux. Assuming that the typical jet angle is $\sim 10^\circ$ the rate of \mathcal{L} GRBs for which the neutrino beam is pointed towards Earth is $\sim 0.5 \times 10^{-8} \text{ Mpc}^{-3} \text{ yr}^{-1}$ consistent with the limit derived by Ahlers & Halzen (2014). Thus, \mathcal{L} GRBs are certainly viable candidates for the origin of the observed extra-galactic neutrino flux!

Finally, if \mathcal{L} GRBs harbor the same engine and relativistic jets as LGRBs then they produce the same GW signals (e.g., Kotake, Takiwaki & Harikae 2012; Birnholtz & Piran 2013). A difference is that while LGRBs are always observed close to the jet axis, the line-of-sight to \mathcal{L} GRBs is typically away from that axis. The GW signal from the engine can be slightly stronger along the jet axis (up to a factor of 1.6 compared to an average

line-of-sight observer), if its origin is quadrupole mass inhomogeneity in a rotating disk (Kochanek & Piran 1993). Other axisymmetric GW sources in the engine, such as mass motions and neutrino emission, vanish along the axis and are strong at the equator (Kotake, Takiwaki & Harikae 2012). The signal from the jet acceleration is also anti-beamed and is strongest along the equator (Birnholtz & Piran 2013). Thus, the off-axis viewing angle of typical \mathcal{L} GRBs is probably an advantage for GW detection. The main advantage of \mathcal{L} GRBs is their much higher rate. The volumetric rate of \mathcal{L} GRBs is larger by about an order of magnitude than that of all LGRBs, including those that are unobservable since their gamma-ray beam points away from the Earth. If only LGRBs that points towards earth are considered then the \mathcal{L} GRB rate is higher by almost three order of magnitude. This is important since targeted GW search for GRBs (e.g., following a detection of gamma-rays) is more sensitive than a blind search, increasing the detection volume by a factor of ≈ 3 (Kochanek & Piran 1993). The various predicted GW signals from the engine and the jet are expected to be detectable by future gravitational wave detectors up to a distance of $\sim 100 \text{ Mpc}$. The rate of LGRBs at that distance is too low to allow a reasonable probability for detection. However, about one \mathcal{L} GRB take place every year within a distance of 100 Mpc, making it a promising GW source for future detectors.

7. CONCLUSIONS

This paper analyzes the first day optical/UV light curve of SN 2006aj/ \mathcal{L} GRB 060218 finding that its progenitor has a compact core engulfed by an extended low-mass material. When the information on this structure is combined with the high velocities inferred from the radio emitting material, it implies that the shock breakout form the extended material must produce a gamma-ray signal that is consistent with the observed \mathcal{L} GRB gamma-ray emission. This indicates that the gamma-rays in 2006aj/ \mathcal{L} GRB 060218 are generated by a mildly relativistic shock breakout and it strongly supports the suggestion that the origin of all \mathcal{L} GRBs' high energy emission is a shock breakout.

These results, which are directly based on the observations of SN 2006aj, naturally suggest a picture that unifies LGRBs and \mathcal{L} GRBs, explaining how two types of explosions that are so different in their gamma-ray signature produce very similar SNe. In this picture LGRBs and \mathcal{L} GRBs are two manifestations of a similar core collapse process that leads to a similar SN explosion mechanism and a similar GRB central engine, where the observational outcome depends only on the slight differences in the existence, or the lack of, a low-mass extended envelope. This model also provides a simple explanation to the peculiar velocity profile seen in SNe that are associated with \mathcal{L} GRBs. It also implies that \mathcal{L} GRBs are more promising sources of high energy neutrinos and GWs than LGRBs. \mathcal{L} GRBs are viable candidates as the source of the observed extra-galactic diffuse neutrino flux and are promising GW sources for the next generation GW detectors.

A final comment on the progenitor structure of SN 2006aj. While the SN light curve constrains M_{ext} and R_{ext} it does not strongly constrain its density profile.

jet. Our findings on the progenitor structure of \mathcal{L} GRB 060218 strongly disfavor the model used by Murase & Ioka (2013)

The only requirement is that most of the mass M_{ext} is concentrated near R_{ext} (Nakar & Piro 2014). This is consistent with any density profile $\rho(r)$ where ρr^3 increases with radius at $r < R_{ext}$ and decreases at $r > R_{ext}$. Thus, we cannot determine whether the inferred progenitor structure is in hydrostatic equilibrium or whether the extended material was thrown out to R_{ext} a short time before the explosion. The latter option may be more attractive given that no current stellar evolution model predicts a hydrostatic structure similar to that SN 2006aj for a fully H stripped star, while recently there are several lines of evidence that massive stars go through a strongly enhanced mass-loss episode a short time before they explode (Ofek *et al.* 2013, 2014;

Gal-Yam *et al.* 2014; Svirski & Nakar 2014). Yet, another intriguing speculation is that the progenitor is affected by a binary, or maybe even by a binary merger (e.g., along similar lines to those suggested by Chevalier 2012), that put the extended material at place a short time before the explosion.

This research was partially supported by an ERC starting grant (GRB/SN), ISF grant (1277/13), ISA grant and by the I-CORE Program (1829/12). I thank Amir Levinson, Dan Maoz, Tsvi Piran, Dovi Poznanski and Amiel Sternberg for enlightening discussions.

REFERENCES

- Aartsen, M. G. *et al.* 2014a, Physical Review Letters, 113(10), 101101, 1405.5303.
Aartsen, M. G. *et al.* 2014b, ArXiv e-prints, 1412.6510.
Ahlers, M. and Halzen, F. 2014, Phys. Rev. D. , 90(4), 043005, 1406.2160.
Ando, S. *et al.* 2013, Reviews of Modern Physics, 85, 1401, 1203.5192.
Barniol Duran, R., Nakar, E., Piran, T., and Sari, R. 2014, ArXiv e-prints, 1407.4475.
Bersten, M. C. *et al.* 2012, ApJ , 757, 31, 1207.5975.
Birnholtz, O. and Piran, T. 2013, Phys. Rev. D. , 87(12), 123007, 1302.5713.
Bromberg, O., Nakar, E., and Piran, T. 2011, ApJL , 739, L55, 1107.1346.
Bromberg, O., Nakar, E., Piran, T., and Sari, R. 2011, ApJ , 740, 100, 1107.1326.
Budnik, R., Katz, B., MacFadyen, A., and Waxman, E. 2008, ApJ , 673, 928, 0705.0041.
Campana, S. *et al.* 2006, Nature , 442, 1008, astro-ph/0603279.
Chevalier, R. A. 2012, ApJL , 752, L2, 1204.3300.
Gal-Yam, A. *et al.* 2014, Nature , 509, 471, 1406.7640.
Hoffich, P., Langer, N., and Duschinger, M. 1993, A&A , 275, L29.
Hümmer, S., Baerwald, P., and Winter, W. 2012, Physical Review Letters, 108(23), 231101, 1112.1076.
Kaneko, Y. *et al.* 2007, ApJ , 654, 385, arXiv:astro-ph/0607110.
Katz, B., Budnik, R., and Waxman, E. 2010, ApJ , 716, 781, ArXiv e-prints 0902.4708.
Kochanek, C. S. and Piran, T. 1993, ApJL , 417, L17, astro-ph/9305015.
Kotake, K., Takiwaki, T., and Harikae, S. 2012, ApJ , 755, 84, 1205.6061.
Kulkarni, S. R. *et al.* 1998, Nature , 395, 663.
Levinson, A. and Bromberg, O. 2008, Physical Review Letters, 100(13), 131101, 0711.3281.
Li, L. 2007, MNRAS , 375, 240, arXiv:astro-ph/0605387.
Liu, R.-Y., Wang, X.-Y., and Dai, Z.-G. 2011, MNRAS , 418, 1382, 1108.1551.
Matzner, C. D. 2003, MNRAS , 345, 575, astro-ph/0203085.
Matzner, C. D. and McKee, C. F. 1999, ApJ , 510, 379, arXiv:astro-ph/9807046.
Mazzali, P. A. *et al.* 2006, Nature , 442, 1018, astro-ph/0603567.
Mazzali, P. A. *et al.* 2007, ApJ , 661, 892, astro-ph/0703109.
Melandri, A. *et al.* 2014, A&A , 567, A29, 1404.6654.
Mirabal, N., Halpern, J. P., An, D., Thorstensen, J. R., and Terndrup, D. M. 2006, ApJL , 643, L99, astro-ph/0603686.
Mizuta, A. and Aloy, M. A. 2009, ApJ , 699, 1261, 0812.4813.
Modjaz, M. *et al.* 2006, ApJL , 645, L21, astro-ph/0603377.
Morsony, B. J., Lazzati, D., and Begelman, M. C. 2007, ApJ , 665, 569, astro-ph/0609254.
Murase, K. and Ioka, K. 2013, Physical Review Letters, 111(12), 121102, 1306.2274.
Murase, K., Ioka, K., Nagataki, S., and Nakamura, T. 2006, ApJL , 651, L5, astro-ph/0607104.
Nakar, E. and Piro, A. L. 2014, ApJ , 788, 193, 1401.7013.
Nakar, E. and Sari, R. 2010, ApJ , 725, 904, 1004.2496.
Nakar, E. and Sari, R. 2012, ApJ , 747, 88, 1106.2556.
Ofek, E. O. *et al.* 2013, Nature , 494, 65, 1302.2633.
Ofek, E. O. *et al.* 2014, ApJ , 789, 104, 1401.5468.
Pian, E. *et al.* 2006, Nature , 442, 1011, astro-ph/0603530.
Piran, T. 2004, Reviews of Modern Physics, 76, 1143, astro-ph/0405503.
Piro, A. L. and Nakar, E. 2013, ApJ , 769, 67, 1210.3032.
Sakurai, A. 1960, Communications on Pure and Applied Mathematics, 13, 353.
Soderberg, A. M. *et al.* 2006, Nature , 442, 1014, astro-ph/0604389.
Sollerman, J. *et al.* 2006, A&A , 454, 503, astro-ph/0603495.
Svirski, G. and Nakar, E. 2014, ApJL , 788, L14, 1403.3400.
Tan, J. C., Matzner, C. D., and McKee, C. F. 2001, ApJ , 551, 946, arXiv:astro-ph/0012003.
Šimon, V., Pizzichini, G., and Hudec, R. 2010, A&A , 523, A56.
Wanderman, D. and Piran, T. 2010, MNRAS , 406, 1944, 0912.0709.
Waxman, E. and Bahcall, J. 1997, Physical Review Letters, 78, 2292, astro-ph/9701231.
Waxman, E., Mészáros, P., and Campana, S. 2007, ApJ , 667, 351, arXiv:astro-ph/0702450.
Woosley, S. E. and Bloom, J. S. 2006, ARAA , 44, 507, astro-ph/0609142.
Zhang, W., Woosley, S. E., and MacFadyen, A. I. 2003, ApJ , 586, 356, astro-ph/0207436.

APPENDIX

THE POWER SOURCE OF THE FIRST OPTICAL PEAK

The analysis of the progenitor structure of SN 2006aj relies on the identification of the first optical/UV peak as a cooling envelope emission. Here this identification is justified by considering known and speculated emission power sources in SNe and GRBs. The conclusion is that while cooling envelope emission provides a natural explanation for the first peak (as discussed in length in Nakar & Piro 2014), all other sources are either ruled out or are highly unlikely.

Cooling envelope: The energy source of cooling envelope emission is the shock that crosses the star and any surrounding mass, if it exists, in regions where the diffusion time is longer than the expansion dynamical time. In these regions the internal energy deposited by the shock is trapped by the gas and it cools adiabatically during the gas expansion, hence the term “cooling envelope”. As the outflow expands its optical depth drop and so does the radiation diffusion time to the observer, while the expansion time grows. In regions where the two time scales become comparable the radiation escapes to the observer. As discussed in Nakar & Piro (2014) this source of emission provides a natural explanation for the first optical peak observed on a time scale of \sim day in case of a double peaked SNe. Important supporting evidence for that in the case of SN 2006aj is the very blue color of the first peak and the fact that the

colors do not vary with time, which indicates that the band that we observe are most likely on the Rayleigh-Jeans part of a blackbody spectrum. This is expected for cooling envelope emission, where the optical depth at the source is high and the radiation has enough time to achieve thermal equilibrium before it escapes, even if the outflow is fast, after the ejecta expanded considerably (Nakar & Sari 2010).

Radioactive decay of ^{56}Ni : This power source of energy, which dominates many SNe light curves, deposits energy at the known decay rate of ^{56}Ni , first to ^{56}Co and then to ^{56}Fe . The observed luminosity from ^{56}Ni is the energy deposited by radioactive decay in “exposed” regions, from where radiation can escape over a dynamical time. Since the total amount of mass in exposed regions depends on time and velocity, the evolution of luminosity generated by ^{56}Ni for a given outflow is set by the fraction of ^{56}Ni in that region (Piro & Nakar 2013). This sets, at any given time, a maximal luminosity that ^{56}Ni can produce, which is the luminosity of an outflow that is composed purely of ^{56}Ni . The exposed mass at the first peak is $\sim 0.01(v/0.2c)M_{\odot}$ implying that the maximal contribution of ^{56}Ni to the luminosity at this time is $\sim 10^{42}(v/0.2c)$ erg/s. This rules out ^{56}Ni as the source of the first peak which show a luminosity $> 3 \times 10^{44}$ erg/s.

Interaction (afterglow): Another power source seen in some SNe is a continuous interaction with the circum-stellar medium. In GRBs such interaction is the source of the afterglow. The difference between continuous interaction and cooling envelope emission is that in the former the shock takes place in a region with optical depth that allows for radiation to escape immediately over a dynamical time scale. Thus, if the first peak is generated by interaction then its luminosity is limited by the instantaneous strength of the interaction. Namely, the explosion ejecta must drive a strong shock into the circum-stellar medium at least up to $t \approx 10$ hr, at which point either the interaction dies (e.g., due to a sharp drop in the circum-stellar density) or the shock becomes radiatively inefficient. The radio emission at $t = 1.89$ day is presumably generated by such interaction and it shows that the interaction shock is propagating at a velocity close to the speed of light (Soderberg *et al.* 2006). The interaction at this point is much too weak to account for the optical emission at this epoch, but assuming that at $t \approx 10$ hr the interaction have been much stronger, could it then be the source of the optical/UV? Considering all the outcomes of the entire allowed phase space for interaction is beyond the scope of this paper, however several general considerations show that it is highly unlikely that interaction can produce the observed first optical/UV peak for two reasons - it predicts an optical/UV spectrum that is too red and an X-ray flux that is too bright compared to the observations.

As the interaction shock is mildly relativistic its radius at the first peak is $r \sim 10^{15}$ cm. The circum-stellar medium must be optically thin for Thomson scattering at this radius, otherwise the mildly relativistic shock breakout would have been taken place at $\sim 10^{15}$ cm, resulting in a much brighter and longer signal in gamma-rays than observed (equation 3). Emission from optically thin mildly relativistic shocks are seen in late stages of GRBs and in some SNe. In these cases the shock is collisionless and it generates strong magnetic fields and accelerates electrons to a power-law distribution. As a result the dominant emission is synchrotron and the spectrum above the self absorption frequency (which is typically in the radio or mm bands) is a power-law that is spread over many orders of magnitude in frequency with a specific flux $F_{\nu} \propto \nu^{\alpha}$ with $\alpha \approx -1$. This is very different than the observed UV spectrum where $\alpha \approx 2$, which requires the self-absorption frequency to be $\gtrsim 10^{15}$ Hz. However, even the highest possible circum-stellar density that is optically thin for Thomson scattering at $\sim 10^{15}$ cm does not bring the synchrotron (or free-free) self-absorption frequency of a mildly relativistic shock into the UV. In addition, the synchrotron power-law spectrum also predicts an X-ray luminosity that is comparable or larger than the UV luminosity, regardless of the location of the self-absorption frequency. In reality at the time of the first peak the X-ray luminosity is fainter than the UV by two orders of magnitude.

Continuous central engine activity: The last power source that is often considered in GRBs and sometimes also in SNe is a continuous energy supply by a central engine, possibly an accreting black-hole or a long lived magnetar. The existence of such sources in SNe is still rather hypothetical, while in GRBs there is stronger evidence that the central engine can be active also on time scales of hour or days. Nevertheless, the optical emission is highly unlikely to be powered this way. The reason is that the bulk of the SN ejecta mass, $\sim 2M_{\odot}$, lies between the center of the explosion and the observer. The photons observed in the first optical peak must be generated at larger radius than that of the bulk of the ejecta. If the energy from the central engine is deposited first in the $\sim 2M_{\odot}$ ejecta it is converted to kinetic and thermal energy of the ejecta before radiated away after the ejecta optical depth drops, over time scale of weeks. Thus, similarly to LGRBs, the energy generated by the central engine must “penetrate” through the bulk of the mass before being dissipated to optical/UV photons. Again, like in LGRBs, this may be done if the engine continuously launches relativistic jets. However, based on GRB observations, the expected optical/UV/X-ray emission from relativistic jets suffers from the same problems of interaction emission. It usually show a power-law spectrum with $\alpha \ll 2$, which does not fit the observed optical/UV spectrum and the faint X-ray emission. More importantly, a relativistic jet must open a cavity in the SN ejecta inducing strong spherical asymmetry in the slow moving material, which is ruled out by the lack of polarization and by the spectral line profiles seen in the SN nebular phase (Mazzali *et al.* 2007).

JET PROPAGATION IN THE CORE AND IN THE EXTENDED MATERIAL

The general physics of a relativistic hydrodynamical jet that propagates in a surrounding medium is described at length in Bromberg *et al.* (2011). Here we provide a brief outline of this system, focusing on the time that the engine must work for the jet to penetrate through the core and through the extended material. A jet that propagates in surrounding media forms a forward-reverse shock structure at its head. The high pressure plasma in the jet head spills

sideways continuously as the jet propagates forming a hot cocoon that engulfs the jet. This cocoon may or may not collimate the jet, depending on the jet and the external medium properties. Since energy is leaving the jet head into the cocoon continuously, the head propagation depends on a continuous supply of energy, which is injected into the head by the jet via the reverse shock. Thus, in order for the jet to propagate a given distance the engine that launches the jet must work for a duration that is long enough so a fresh jet material will continue to cross the reverse shock during the entire propagation. Thus, if the head propagates up to a distance r at a velocity $\beta_h c$ the jet working time must be:

$$t_{eng}(r) \approx \frac{r}{c\beta_h}(1 - \beta_h) \quad (\text{B1})$$

where the term $1 - \beta_h$ includes the relative velocity between the relativistic jet and the head. This term is ≈ 1 for a Newtonian head, implying that the engine working time is simply the jet propagation time. However, if the head is relativistic then by the time that the engine stops working the head is at a distance $\approx ct_{eng}$ from the center and the last jet element that was launched by the engine will catch up with the head only after $t_{eng}/(1 - \beta_h)$. During that time the jet will continue to drive the head forward. Thus, the engine working time needed for a relativistic head to propagate a distance r is much shorter than r/c .

The evolution of the jet is determined by finding the properties of the various components (e.g., head, cocoon, etc.) of that system. The propagation velocity of the head is set by the balance of the jet luminosity per unit area into the head and the ram pressure of the ambient medium. It is therefore useful to define a dimensionless parameter which is the ratio between the energy density of the jet and the rest-mass energy density of the ambient medium (Matzner 2003)

$$\tilde{L} = \frac{L_j}{\Sigma_j \rho c^3}, \quad (\text{B2})$$

where L_j is the total jet luminosity, Σ_j is the jet cross-section at the head and ρ is the ambient medium density at the head location. The propagation velocity of the jet head is:

$$\beta_h = \frac{1}{1 + \tilde{L}^{-1/2}}. \quad (\text{B3})$$

Thus, the head is relativistic when $\tilde{L} \gg 1$ and Newtonian for $\tilde{L} \ll 1$. The collimation of the jet depends also on the half opening angle at which the jet is launched, θ_0 , where for $\tilde{L} < \theta_0^{-4/3}$ the jet is collimated by the cocoon pressure. The jet collimation affects the value of Σ_j and thus also the value of \tilde{L} . For a given set of parameters Bromberg *et al.* (2011) obtain:

$$\tilde{L} = \begin{cases} \left(\frac{L_j}{\rho t^2 \theta_0^4 c^5} \right)^{2/5} & \tilde{L} < \theta_0^{-4/3} \text{ (Collimated)} \\ \frac{L_j}{\rho t^2 \theta_0^2 c^5} & \tilde{L} > \theta_0^{-4/3} \text{ (Uncollimated)} \end{cases} \quad (\text{B4})$$

where t is the time since the jet launching started and ρ is the external density near the jet head location. Equations B3 and B4 together can be solved to find the jet location at time t .

The isotropic equivalent luminosity of a typical GRB jet is $L_{iso} \sim 10^{51}$ erg/s and its opening angle is $\theta_0 \sim 10^\circ$. The beaming corrected jet luminosity is then $L_j = L_{iso} \theta_0^2 / 2$. In a massive ($M_{core} > M_\odot$) and compact ($R_{core} \sim 10^{11}$ cm) core the density is high and $\tilde{L} \lesssim 1$, resulting in a Newtonian (or at most a mildly relativistic) collimated jet. Thus, the engine working time must be comparable to the time needed for the jet to cross the core:

$$t_{eng,core} \sim 7 \left(\frac{L_{iso}}{10^{51} \text{ erg s}^{-1}} \right)^{-1/3} \left(\frac{\theta_0}{10 \text{ deg}} \right)^{2/3} \left(\frac{R_{core}}{10^{11} \text{ cm}} \right)^{2/3} \left(\frac{M_{core}}{10 M_\odot} \right)^{1/3} \text{ s}. \quad (\text{B5})$$

Here we used the approximation $\beta_h \approx \tilde{L}^{1/2}$ which is appropriate for Newtonian heads.

The density of the extended material is much lower than in the core. As a result, for a typical GRB jet $\tilde{L} > \theta_0^{-4/3}$, resulting in an uncollimated relativistic jet. The minimal engine working time for a successful jet penetration is shorter than the extended material light crossing time, but it is still much longer than the time it takes the jet to cross the core:

$$t_{eng,ext} \sim 150 \left(\frac{L_{iso}}{10^{51} \text{ erg s}^{-1}} \right)^{-1/2} \left(\frac{R_{ext}}{3 \times 10^{13} \text{ cm}} \right)^{1/2} \left(\frac{M_{ext}}{10^{-2} M_\odot} \right)^{1/2} \text{ s}. \quad (\text{B6})$$

where we used the approximation for a relativistic head $\gamma_h \approx \tilde{L}^{1/4} / \sqrt{2}$, where γ_h is the head Lorentz factor.